bioRxiv preprint doi: https://doi.org/10.1101/2020.04.21.054155; this version posted April 23, 2020. The copyright holder for this preprint (which was not certified by peer review) is the author/funder, who has granted bioRxiv a license to display the preprint in perpetuity. It is made available under aCC-BY-NC-ND 4.0 International license.

Electrical Oscillations of Brain Microtubules

Brenda C. Gutierrez, Horacio F. Cantiello and María del Rocío Cantero*

Laboratorio de Canales Iónicos, Instituto Multidisciplinario de Salud, Tecnología y Desarrollo (IMSaTeD, UNSE-CONICET)

Running Title: *Electrical activity of brain microtubules*

Keywords: Microtubule, Tubulin, Electrical Oscillations, Brain

*Address correspondence to: María del Rocío Cantero, Laboratorio de Canales Iónicos, Instituto Multidisciplinario de Salud, Tecnología y Desarrollo (IMSaTeD, UNSE-CONICET), RN 9 km 1125, El Zanjón, Santiago del Estero, Argentina (4206).

Tel: +54 (11) 6580-4629; Email: mdrcantero@gmail.com

Significance Statement. Microtubules (MTs) are important cytoskeletal structures engaged in a number of specific cellular activities. Recent in vitro electrophysiological studies indicate that different brain MT structures, including two-dimensional sheets and bundles, generate highly synchronous electrical oscillations. However, no information has been heretofore available as to whether isolated MTs also engage in electrical oscillations. In the present study, a broader spectrum of fundamental frequencies was always observed in isolated MTs as compared to the MT sheets. This interesting finding is consistent with the possibility that more structured MT complexes (i.e. bundles, sheets) may render more coherent response at given oscillatory frequencies and raise the hypothesis that combined MTs may tend to oscillate and entrain together. The present study provides to our knowledge the first experimental evidence for electrical oscillations of single brain MTs.

Abstract. Microtubules (MTs) are important cytoskeletal structures engaged in a number of specific cellular activities, including vesicular traffic and motility, cell division, and information transfer within neuronal processes. MTs also are highly charged polyelectrolytes. Recent in vitro electrophysiological studies indicate that different brain MT structures, including two-dimensional (2D) sheets (MT sheets) and bundles, generate highly synchronous electrical oscillations. However, no information has been heretofore available as to whether isolated MTs also engage in electrical oscillations, despite the fact that taxol-stabilized isolated MTs are capable of amplifying electrical signals. Herein we tested the effect of voltage clamping on the electrical properties of isolated non-taxol stabilized brain MTs. Electrical oscillations were observed on application of holding potentials between ±200 mV that responded accordingly with changes in amplitude and polarity. Frequency domain spectral analysis of time records from isolated MTs disclosed a richer oscillatory response as compared to that observed in voltage clamped MT sheets from the same preparation. The data indicate that isolated brain MTs are electrical oscillators that behave as "ionic-based" transistors whose activity may be synchronized in higher MT structures. The ability of MTs to generate, propagate, and amplify electrical signals may have important implications in neuronal computational capabilities.

Introduction

MTs are long hollow cylinders assembled from αβ-tubulin dimer subunits (1-3). It has been long recognized that MTs play an essential role in eukaryote vesicle trafficking and cell division, and in neurons MTs contribute to the development of neuronal structures, including axons and dendrites (4, 5), and may be implicated in cognitive processing (6). The MT-associated proteins tau and MAP2 are involved in such neuronal processes as learning and memory (7-9), and MTs have also been linked to ion channel regulation, thus contributing to the electrical activity of excitable cells (10) and the

bioRxiv preprint doi: https://doi.org/10.1101/2020.04.21.054155; this version posted April 23, 2020. The copyright holder for this preprint (which was not certified by peer review) is the author/funder, who has granted bioRxiv a license to display the preprint in perpetuity. It is made available under aCC-BY-NC-ND 4.0 International license.

processing of electrical signals within neurons (11, 12). Previous studies by ours and other groups had determined both experimentally and theoretically the ability of MTs to act as a nonlinear transmission lines capable of electrical signal amplification (13-17). More recent studies from our laboratory demonstrated that different tubulin structures including mammalian brain MT sheets and bundles generate strong electrical oscillations (18, 19). The electrical behavior of MT sheets is mechanistically consistent with organic electrochemical transistors that support both amplification and self-sustained current- (and voltage-) oscillations (18-20). In this model, a gate region of the electrochemical transistor would drive the synchronous open-close cycles of ion-permeable nanopores that elicit an electrodiffusional circuit. From a structural viewpoint, this electrical activity may be linked to the nature of the ensemble of the MT subunits. The MT surface forms different structural lattices that generate by lateral apposition of protofilaments at least two types of nanopores, at either αβ interdimer interfaces, or αβ intradimer interfaces (21, 22), such that the observed electrical phenomenon would implicate changes in nanopore conductance (18). Despite the fact that the hypothesis will require further investigation, we recently obtained experimental evidence that non-oscillating MT sheets display properties of memristive devices that may underlie the gating mechanism of the MT conductance (20).

To gain further insight into the electrical oscillatory activity of different brain MT structures, in the present study, we explored the ability of single MTs to handle electrical signals. To attain this goal, the loose-clamp configuration of the voltage clamp technique was applied to non-taxol stabilized purified isolated MTs. In symmetrical high ionic strength conditions, with 140 mM KCl solution, voltage clamped MTs, generated electrical oscillations at holding potentials different from zero mV. Spontaneous changes in amplitude and frequency were observed in response to the magnitude and polarity of the driving electrical force. Isolated MTs held qualitatively similar electrodynamic properties as previously reported MT structures (18-20), suggesting that intracellular electrical signaling may heavily obey to the assembly and organization of the various cytoskeletal structures, which in the case of MTs may rely on the activity of surface nanopores (18-21). The data indicate, however, that the spectral oscillatory behavior of isolated MTs may be richer and more chaotic than that of MT sheets, suggesting that MTs organization may induce a strong coherence in the fundamental frequencies in the oscillations. Frequency domain driven electrical information may depend on the structural dynamics of MTs assemblies.

Materials & Methods

Preparation of isolated MTs. Commercially available, purified tubulin from bovine brain was utilized in the present study (catalog No. T238, Cytoskeleton, Denver, CO). Tubulin was polymerized with a "hybrid" protocol in the absence of taxol, following loosely general guidelines from the Mitchinson Lab's online protocols (http://mitchison.med.harvard.edu/protocols/). Briefly, all reactions were conducted in BRB80 solution, containing 80 mM PIPES (1, 4-piperazinediethanesulfonic acid), 1 mM $MgCl_2$, 1 mM EGTA, and pH 6.8 with KOH. In some experiments, an aliquot of the tubulin-containing solution was mixed with 2 µl glycerol, 1 mM dithiothreitol (DTT) and 1 mM GTP and incubated for 5 min at room temperature. No significant differences were observed under different incubation conditions. Isolated MTs were immunochemically labeled with anti α-tubulin antibody, as previously reported (19). The primary antibody used was raised in rabbit against amino acids 149-448 of human α-tubulin was obtained (H-300, sc-5546, Santa Cruz Biotechnology Inc) and used at 1:500 dilution. The secondary antibody used for tubulin staining was an FITC-tagged bovine anti-rabbit IgG-R (sc-2367, Santa Cruz Biotechnology Inc, CA) used at a 1/1000 dilution. Samples were viewed under DIC and fluorescence microscopy with an inverted Olympus IX71 microscope connected to a digital CCD camera C4742-80-12AG (Hamamatsu Photonics KK, Bridgewater, NJ). Images were collected with the IPLab Spectrum (Scanalytics, Viena, VA) acquisition and analysis software, running on a Dell-NEC personal computer.

bioRxiv preprint doi: https://doi.org/10.1101/2020.04.21.054155; this version posted April 23, 2020. The copyright holder for this preprint (which was not certified by peer review) is the author/funder, who has granted bioRxiv a license to display the preprint in perpetuity. It is made available under aCC-BY-NC-ND 4.0 International license.

Electrophysiological data acquisition and analysis of isolated MTs and MT sheets. The electronic setup to obtain electrical recordings from voltage-clamped MTs consisted of a conventional patch clamping amplifier (Axopatch 200B, Molecular Devices, Sunnyvale CA), directly connected to the MT sample via a saline-containing patch pipette, as previously reported (18, 19). Patch pipettes were made from soda lime capillary tubes (Biocap, Buenos Aires, Argentina) with 1.25 mm internal diameter and a tip diameter of ~4 µm. Pipette tips most often rendered resistances in the order of 4-15 MΩ in an "intracellular" KCl solution containing, in mM: KCl 140, NaCl 5, EGTA 1.0, and Hepes 10, adjusted to pH 7.18 with KOH. To initiate the experiment, isolated MTs in the preparation (Fig. 1b) were identified both in DIC and fluorescence, approached by the patch pipette, and attached by light suction from the pipette tip (Fig. 1a, c). Voltage clamp protocols only included steady steps at various holding potentials (gap-free protocol), from zero mV. Because the loose-patch-clamp configuration was applied in most experiments, the command voltage (V_{cmd}) applied through the amplifier, would differ from the tip potential "seen" by the MT surface. This difference depended on the magnitude of the seal resistance. Voltage corrections under "loose clamp" configuration were conducted as described in (19). Electrical signals were acquired and filtered at 10 kHz, digitized with an analog-digital converter (Digidata 1440A, Molecular Devices) and stored in a personal computer with the software suite pCLAMP 10.0 (Molecular Devices), also used for data analysis. Sigmaplot Version 11.0 (Jandel Scientific, Corte Madera, CA) was used for statistical analysis and graphics.

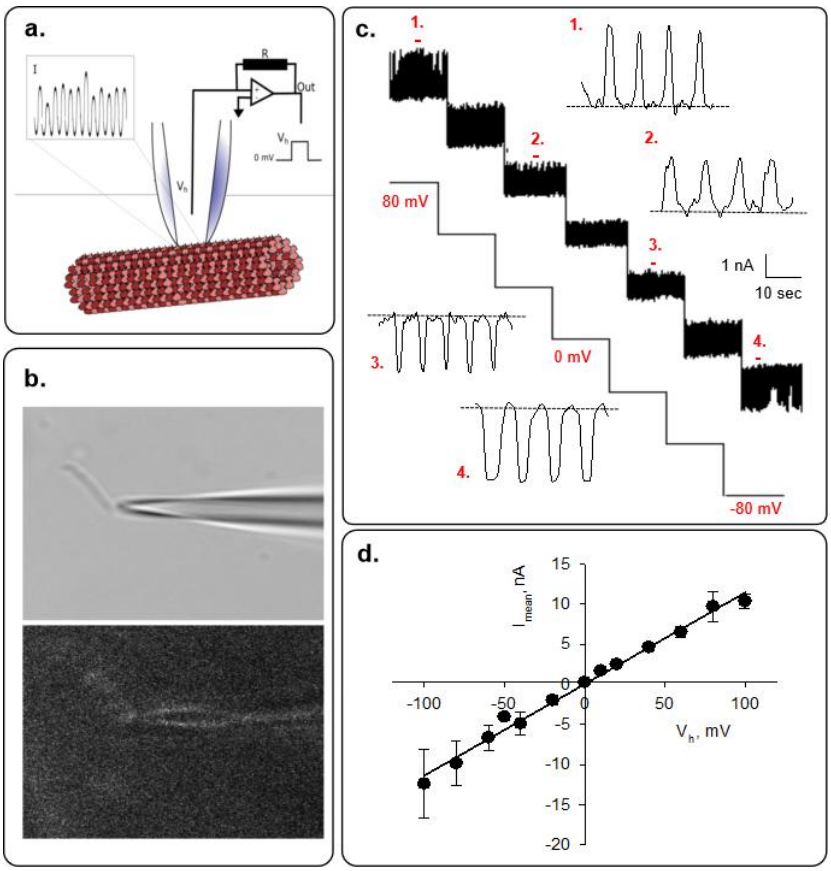

Fig. 1: *Experimental setup and electrical recordings from isolated brain microtubules.* (**a**) Schematics of the patch-clamp configuration used to record electrical oscillations from isolated brain MTs. (**b**) (*Top Panel*), DIC image of patch pipette closing in on an isolated MT, which was fluorescently labeled with an FITC-anti-α-tubulin antibody complex (*Bottom Panel*) x60. (**c**) Electrical recordings at different holding potentials (±80 mV) as indicated. Expanded electrical oscillations shown correspond to regions numbered "1" through "4". Please note that voltage values represented the driving potentials at the patch clamp amplifier and the values sensed at the MT surface. (d) Mean current-to-voltage relationship obtained in symmetrical KCl. Data are representative of n = 3 experiments.

Other current analyses. Unless otherwise stated, electrical tracings shown throughout the study were unfiltered data. Average currents were obtained by integration of one-second tracings expressed as mean ± SEM values, where (*n*) represented the number of experiments analyzed for a given condition. Power spectra of unfiltered data were obtained by the Fourier transform subroutine of Clampfit 10.0. Limit cycles were constructed by the time delay (τ) approach from unfiltered tracings, where the lag

bioRxiv preprint doi: https://doi.org/10.1101/2020.04.21.054155; this version posted April 23, 2020. The copyright holder for this preprint (which was not certified by peer review) is the author/funder, who has granted bioRxiv a license to display the preprint in perpetuity. It is made available under aCC-BY-NC-ND 4.0 International license.

time τ was chosen arbitrarily at $2f$, where f was data acquisition sampling frequency (17). Three dimensional phase space diagrams were constructed in Sigmaplot 11.0.

Solutions and chemicals used in electrophysiological experiments. All reagents were obtained from Sigma-Aldrich (St Louis MI, USA).

Results & Discussion

The present study, was conducted to obtain electrical recordings from isolated MTs made from purified commercial tubulin with a protocol that avoided the use of the MT stabilizer taxol, which is a specific inhibitor of the electrical oscillations of MT sheets (17), and may explain previous failure to observe electrical oscillations in isolated MTs (13, 15). The experiments described herein were conducted with the "loose" patch clamp configuration under symmetrical ionic conditions, namely identical saline composition in both patch pipette and bath, with an "intracellular-like" Ca^{2+}-free solution containing high KCl (140 mM) and 1 mM EGTA (see Materials & Methods). Isolated MTs were visualized and identified under combined DIC and fluorescent microscopy by exposure of the MT preparation to both a primary anti α-tubulin antibody and an FITC-fluorescent secondary antibody to the (Fig. 1b, c).

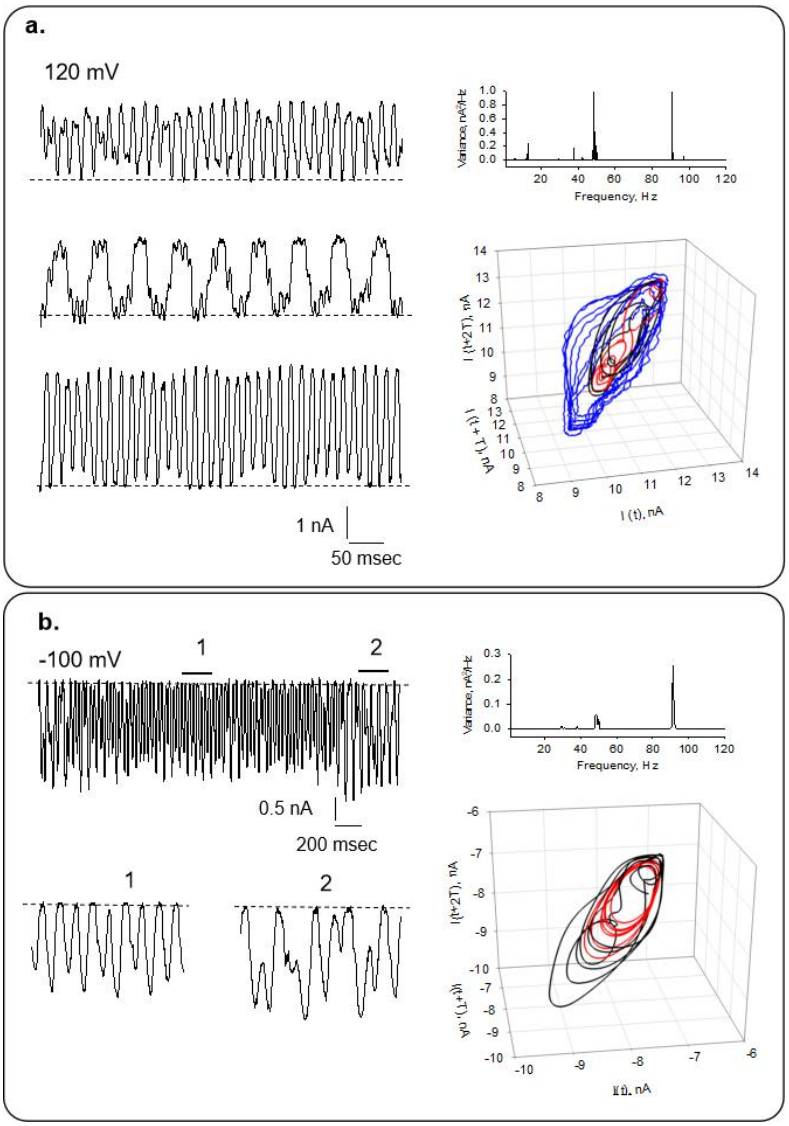

Fig 2: *Current oscillations of voltage-clamped brain microtubules at holding potentials of different polarity*. (**a**) *Left.* Example of changes observed in oscillatory behavior from an isolated MT at a positive holding potential, 120 mV. From Top to Bottom, the tracings represent different instances of the same record. Data were obtained in symmetrical KCl solution (140 mM). *Right*. (*Top*) The panel shows the power spectrum from the oscillatory currents shown in tracings on Left. (*Bottom*) 3D Poincaré map of time derivatives from the tracing shown in (**a**). Black, red and blue lines correspond to Top, Middle and Bottom tracings, respectively. (**b**) *Left.* Representative recording of an isolated MT showing changes in the pattern of oscillations at bottom panels (1 & 2) at a negative holding potential, -100 mV. *Right*. (*Top*) Power spectrum from oscillatory currents corresponding to the tracing shown on Left. 3D Poincaré map of time derivatives of tracings (*Bottom*). Red and black lines correspond to "1" and "2", as indicated in the electrical recording.

bioRxiv preprint doi: https://doi.org/10.1101/2020.04.21.054155; this version posted April 23, 2020. The copyright holder for this preprint (which was not certified by peer review) is the author/funder, who has granted bioRxiv a license to display the preprint in perpetuity. It is made available under aCC-BY-NC-ND 4.0 International license.

Electrical activity of isolated microtubules

Isolated MTs were approached with the patch pipette connected to a patch clamp amplifier as indicated in Fig. 1a. Experiments were conducted with small tipped (4 μm^2) pipettes. Apposition of the pipette tip onto an MT (Fig. 1b) only increased the seal resistance in 1.24 ± 0.29 MΩ reaching to 12.84 ± 5.20 MΩ, n = 14, Median 6.50 MΩ, and a range of 2.83 M Ω to 63.3 MΩ, in contrast to the high seal resistance usually obtained with MT sheets (18). This approach rendered a type of loose patch configuration as previously used with brain MT bundles (19). Isolated MTs were initially voltage-clamped at a holding potential of zero mV showing no electrical activity in any successful experiments (n = 14). Voltage-clamped MTs displayed spontaneous, self-sustained electrical oscillations (20/29) (Figs. 1a & 2) that responded directly to the magnitude and polarity of the electrical stimulus. The spontaneous oscillations showed changes in regime, particularly by changes in polarity of the holding potential (Fig. 1c). Mean values of the oscillatory currents showed a linear response with respect to holding potential (Fig. 1d), with a change in conductance of 59.6 ± 3.6 nS (n = 3). After loose-patch corrections, the change in conductance was 160.8 ± 7.6 nS (n = 3), which represents a much higher change in conductance that previously reported for more complex MT structures (18, 19) The electrical activity consisted of synchronous oscillations that changed in both amplitude and frequency (Fig. 2) in the absence of any changes in driving force. Fundamental frequencies were often seen at 13, 29, 38, 48, and 90 Hz (Fig. 2 a & b). At a given holding potential, oscillations spontaneously changed with time, both in amplitude and the pattern of frequencies (Figs. 2a & b). An increase in the magnitude of the holding potential increased the amplitude of the oscillations, evidencing more frequencies and more complex oscillatory behavior (Fig. 3).

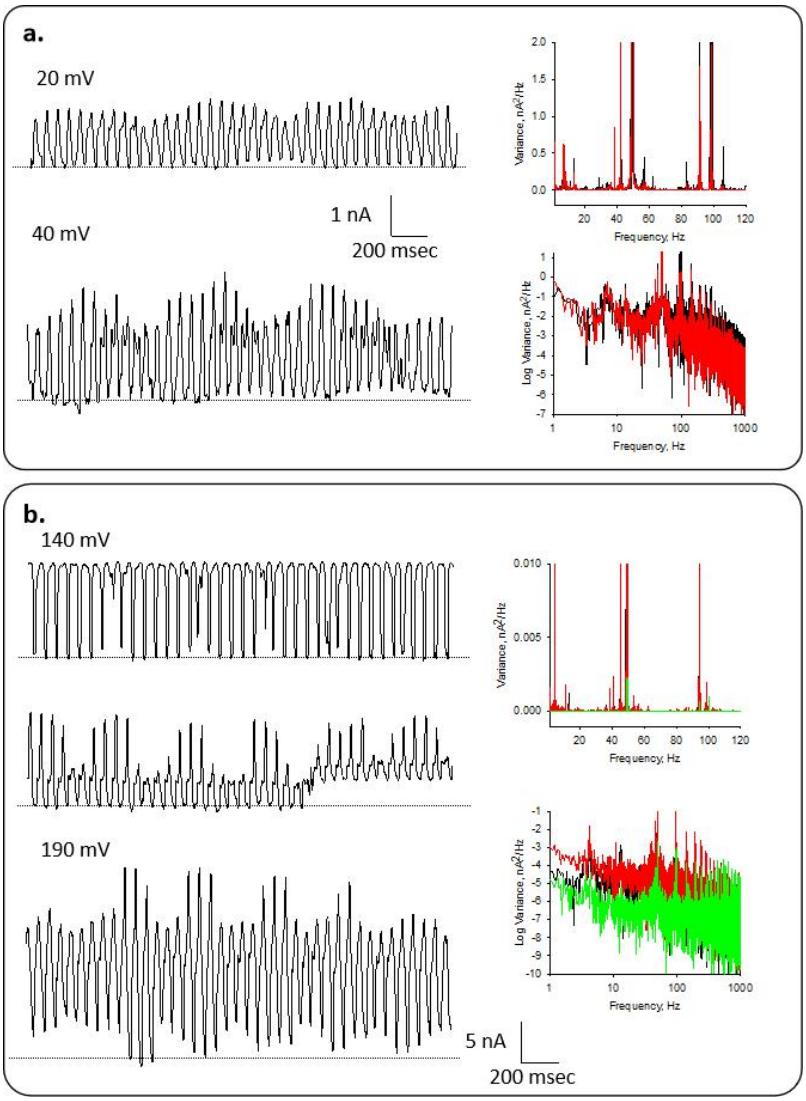

Fig 3: *Different patterns of current oscillations at different holding potentials*. (**a**) *Left*. Representative recording of a voltage-clamped isolated MT in the presence of symmetrical KCl at 20 mV and 40 mV, as indicated. *Right.* Linear-linear (Top) and Log-Log (Bottom) plots of Fourier power spectra obtained from unfiltered current responses of tracings on *Left*. Black and red lines correspond to 20 mV and 40 mV, respectively. (**b**) Representative time series recording of voltage-clamped isolated MT in the presence of symmetrical KCl at 140 mV and 190 mV, as indicated. At 140 mV, the tracings represent different instances of the same record. *Right.* Linear-linear (Top) and Log-Log (Bottom) plots of Fourier power spectra obtained from unfiltered current responses of tracings on *Left*. Black, green and red lines correspond to 140 mV (top tracing), 140 mV (middle tracing) and 190 mV, respectively.

To further explore the rich oscillatory behavior of isolated MTs, similar experiments were

bioRxiv preprint doi: https://doi.org/10.1101/2020.04.21.054155; this version posted April 23, 2020. The copyright holder for this preprint (which was not certified by peer review) is the author/funder, who has granted bioRxiv a license to display the preprint in perpetuity. It is made available under aCC-BY-NC-ND 4.0 International license.

conducted under identical conditions, including the same pipette before and after attachment to either MT sheets, or isolated MTs present in the same preparation (Fig. 4). Clearly, the unattached pipette showed a largely white noise spectrum with contaminant line frequency peaks at 50 and 100 Hz (Fig. 4a & d), while MT-attached spectra displayed colored peaks of relevant frequencies in the oscillatory behavior. Clear differences were observed in the MT sheets (n = 4), were it was often found fundamental frequency peaks in the range of 38 and 90 Hz as confirmed by Fourier transformation (Fig. 4b & d). In all cases, isolated MT signals were richer in frequency peaks, as compared to their corresponding MT sheet (Fig. 4c & d). Thus, MTs complex in the larger flat surface of the MT sheets (with tighter seal as well), was usually more coherent in terms of fundamental frequency peaks observed. The data indicated that the electrical oscillations of isolated MTs were qualitatively similar to those observed in more complex MT structures, including 2D sheets (18), and bundles (19). However, an interesting difference became evident, namely, that the richer oscillatory behavior of isolated MTs drastically changed by assembling into flat surfaces that only displayed fewer but stronger oscillatory peaks (Fig. 4).

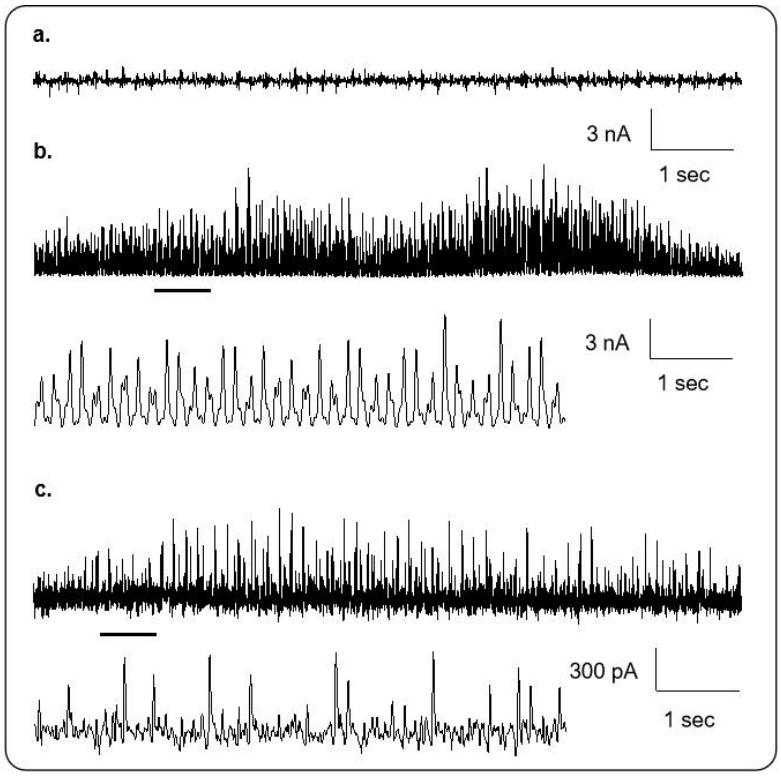

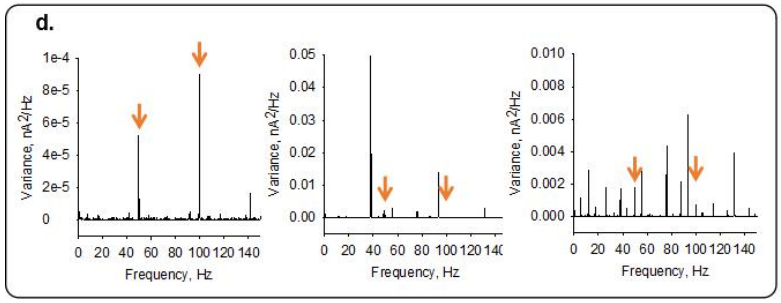

Fig 4: *Differences in the pattern of current oscillations between isolated MTs and MT sheets*. Representative recordings obtained for the pipette in solution (**a**), a voltage-clamped MT (**b**) and an isolated MT (**c**) in the presence of symmetrical 140 mM KCl. Expanded tracings are also shown. (**d**) Linear-linear plots of Fourier power spectra obtained from unfiltered current responses of tracings in (**a**) (Left), (**b**) (Middle), and (**c**) (Right).

Previous studies with taxol-stabilized MTs, originally demonstrated the propagation and amplification of electrical pulses, but not the presence of electrical oscillations (13, 15). In those studies, coupling of the stimulus pipette to one end of the MT increased the overall conductance of the pipette, and coupling to a second pipette at the other end. The MT was able to amplify both the electrical pulse injected at the stimulus as well as the collection sites such that transfer amplification ratios up to 2.35 were observed under high ionic strength conditions (13). The electrical response was linearly dependent on the stimulus pipette input voltage, indicating strictly inverse ohmic response, i.e., linear amplification and was observed in either direction (stimulus by either amplifier). However, these finding never encountered oscillatory responses at either end or the amplification response. In retrospect, the fact that taxol had been used in

bioRxiv preprint doi: https://doi.org/10.1101/2020.04.21.054155; this version posted April 23, 2020. The copyright holder for this preprint (which was not certified by peer review) is the author/funder, who has granted bioRxiv a license to display the preprint in perpetuity. It is made available under aCC-BY-NC-ND 4.0 International license.

the MT preparation to stabilize the MTs and hold them to the pipettes (13, 15) may have accounted for this behavior (lack thereof). Indeed, our more recent observations demonstrated that the electrical oscillations of both MT sheets and bundles were readily inhibited by addition of taxol to the preparation (18, 19). Thus, herein, we explored non-taxol stabilized MTs in this study, with instead made it more difficult to find and handle the isolated MTs in the preparation. Most tubulins formed 2D sheets under the incubation conditions. The reason for this phenomenon is still unclear. Although in the instances where isolated MTs were successfully found and patched, however, the electrical behavior was different to that of the MT sheets, also present in the preparation. It is to note that MT sheets have long being recognized as intermediate structures in MT formation (22). In particular, a broader spectrum of fundamental frequencies was always observed in isolated MTs as compared to the MT sheets. This interesting finding is consistent with the possibility that more structured MT complexes (i.e. bundles, sheets) may render more coherent response at given oscillatory frequencies and raise the hypothesis that combined MTs may tend to oscillate and entrain together. Different oscillatory modes have been postulated for MT structures (23, 24)

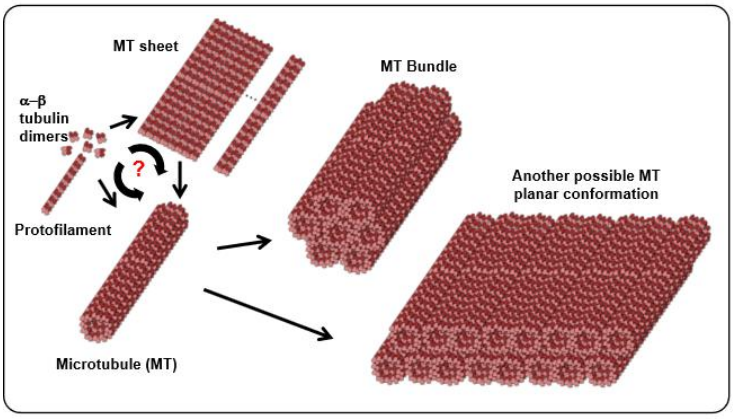

Fig 5: *Diagram of different tubulin assembly conformations during the process of MT formation.* The αβ tubulin dimers (*Left*), arrange in a necklace-type sequence known as a protofilament, which could either curl, or attach to each other to form a MT sheet, which then curves into an MT. Often times lateral apposition of protofilaments spontaneously extends to larger flat surfaces. It was originally postulated that these structures were those used in our recent patch-clamping studies (Cantero 2016). However, MTs may also assemble to form different super structures, including sheets, bundles, or macrotubes, such that the possibility also exists for 2D structures to occur from pre-formed MTs to attach laterally as well as by surface apposition.

In conclusion, the present study provides to our knowledge the first experimental evidence for electrical oscillations of single brain MTs. The data are somewhat analogous to the oscillating behavior of other MT structures (18, 19). However, the electrical behavior of isolated MTs was somewhat richer, and consistent with the presence of several fundamental frequencies that cancel out and disappear to offer more coherent behavior in brain MT sheets. Also consistent with previous findings, it could be postulated that localized changes in electrostatic potentials arising from interactions between the intra- and extra-MT environments of these highly charged polymers to induce oscillatory currents under asymmetric ionic distributions between them. This type of electrical behavior may serve as a novel mechanism for intracellular signaling. MT electrical oscillations in the neuronal environment may provide a novel means for interactions between different cellular organelles and/or cytoskeletal structures as we recently observed in the context of interactions between MT sheets and actin filaments (20). Actin filaments themselves are able to conduct and amplify electrical signals (26, 27) such that electrical information processing in neurons may couple to the gating of cytoskeleton-associated ion channels in such compartments as the nerve´s axon. Finally, the present study sheds new light into the structural/functional correlates of MT electrical oscillations (Fig. 5). Tubulin dimers, arrange in necklace-type sequences known as protofilaments, which either curl, or attach to each other laterally to form a 2D-sheets, which then either curve into MTs, and/or flatten and form floating rafts (22). Although we speculated that lateral apposition of protofilaments spontaneously extends to larger flat surfaces (18), it may have been possible for MTs to assemble and form different super structures such as sheets, bundles, or macrotubes, the possibility also exists for 2D structures from pre-formed MTs to

bioRxiv preprint doi: https://doi.org/10.1101/2020.04.21.054155; this version posted April 23, 2020. The copyright holder for this preprint (which was not certified by peer review) is the author/funder, who has granted bioRxiv a license to display the preprint in perpetuity. It is made available under aCC-BY-NC-ND 4.0 International license.

electrostatically interact and attach laterally as well as by surface apposition (27-29), to form different electrically-active structures instead.

Acknowledgements

The authors wish to acknowledge the Ministerio de Ciencia, Tecnología e Innovación Productiva de la Nación (Argentina) for funding the studies through PICT 2016-3739.

References

1. Dustin, P. 1984. Microtubules. Springer-Verlag, Berlin.

2. Amos, L. A., and W. B. Amos. 1991. Molecules of the Cytoskeleton. Guilford Press, New York. 253 pp.

3. Desai, A., and T.J. Mitchison. 1997. Microtubule polymerization dynamics. Ann Rev. Cell Develop. Biol., 13: 83-117.

4. Conde, C., and A. Cáceres. 2009. Microtubule assembly, organization and dynamics in axons and dendrites. Nature Rev. Neurosci., 10: 319-332.

5. Stiess M, and F. Bradke. Neuronal polarization: the cytoskeleton leads the way. Develop. Neurobiol. 71: 430-444, 2011.

6. Priel, A., Ramos A. J., Tuszynski, J. A., and H. F. Cantiello. 2006. The dendritic cytoskeleton as a computational device: An hypothesis. In "The Emerging Physics of Consciousness". Tuszynski, J. A. Ed. Springer, pp. 293-325.

7. Khuchua, Z., D. F. Wozniak, M. E. Bardgett, Z. Yue, M. McDonald, J. Boero, R. E. Hartman, H. Sims, and A. W. Strauss. 2003. Deletion of the N-terminus of murine MAP2 by gene targeting disrupts hippocampal CA1 neuron architecture and alters contextual memory. Neuroscience, 119: 101-111.

8. Wong, R. W., M. Setou, J. Teng, Y. Takei, and N. Hirokawa. 2002. Overexpression of motor protein KIF17 enhances spatial and working memory in transgenic mice. Proc. Natl. Acad. Sci. USA. 99: 14500-14505.

9. Woolf, N. J., Zinnerman M. D., and G. V. W. Johnson. 1999. Hippocampal microtubule-associated protein-2 alterations with contextual memory. Brain Res. 821:241-249.

10. Johnson, B. D., and L. Byerly. 1994. Ca^{2+} channel Ca^{2+}-dependent inactivation in a mammalian central neuron involves the cytoskeleton. Pflügers Arch., 429:14-21.

11. Johnston, D., Magee, J. C., Colbert, C. M., and B. R. Christie. 1996. Active properties of neuronal dendrites. Annu. Rev. Neurosci., 19: 165-186.

12. Ramon-Moliner, E. 1968. The morphology of dendrites. In The Structure and Function of Nervous Tissue. G. H. Bourne, editor. Academic Press, New York. 205–267.

13. Priel, A., Ramos A. J., Tuszynski, J. A., and H. F. Cantiello. 2006. A biopolymer transistor: electrical amplification by microtubules. Biophys. J., 90: 4639-4643.

bioRxiv preprint doi: https://doi.org/10.1101/2020.04.21.054155; this version posted April 23, 2020. The copyright holder for this preprint (which was not certified by peer review) is the author/funder, who has granted bioRxiv a license to display the preprint in perpetuity. It is made available under aCC-BY-NC-ND 4.0 International license.

14. Priel, A., and J.A. Tuszynski. 2008. A nonlinear cable-like model of amplified ionic wave propagation along microtubules. Europhys. Let., 83: 68004.

15. Priel, A., Ramos, A. J., Tuszynski, J. A., and H. F. Cantiello. 2008. Effect of calcium on electrical energy transfer by microtubules. J. Biol. Phys., 34(5): 475-485.

16. Sekulić, D. L., Satarić, B. M., Tuszynski, J. A., and M. V. Satarić. 2011. Nonlinear ionic pulses along microtubules. Europ. Phys. J. E 34: 49.

17. Henry, R., Durai, K., Net, S., Balraj, A., and W. S. Priya. 2011. Modeling a micro tubule as a diode. J. Biosensors & Bioelectr., 2: 106.

18. Cantero, M. R., Perez, P. L., Smoler, M., Villa Etchegoyen, C., and H. F. Cantiello. 2016. Electrical oscillations in two-dimensional microtubular structures. Sci. Rep., 6: 27143.

19. Cantero, M. R., Villa Etchegoyen, C., Perez, P. L., Scarinci, N., and H. F. Cantiello. 2018. Bundles of brain microtubules generate electrical oscillations. Sci. Rep., 8(1): 11899.

20. Cantero, M.R., Perez, P.L., Scarinci, N., and H.F. Cantiello. 2019. Two-dimensional brain microtubule structures behave as memristive devices. Sci. Rep., 9(1): 12398.

21. Freedman, H., Rezania, V., Priel, A., Carpenter, E., Noskov, S. Y., and J. A. Tuszynski. 2010. Model of ionic currents through microtubule nanopores and the lumen. Phys. Rev. E Stat. Nonlin. Soft Matter Phys., 81(5 Pt 1): 051912.

22. Chrétien, D., Fuller, S. D., and E. Karsenti. 1995. Structure of growing microtubule ends: Two-dimensional sheets close into tubes at variable rates. J. Biol. Chem., 129(5): 1311-1328.

23. Cifra, M., Pokorný, J., Havelka, D., and O. Kucera. 2010. Electric field generated by axial longitudinal vibration modes of microtubule. BioSystems, 100: 122-131.

24. Zhao, Y., and Q. Zhan. 2012. Electric fields generated by synchronized oscillations of microtubules, centrosomes and chromosomes regulate the dynamics of mitosis and meiosis. Theor. Biol. Med. Model., 9: 26.

25. Cantero, M.R., Gutierrez, B.C., and H.F. Cantiello. 2020. Actin filaments modulate electrical activity of brain microtubule protein two-dimensional sheets. Cytoskeleton (Hoboken), 77(3-4): 167-177.

26. Lin, E. C., and H. F. Cantiello. 1993. A novel method to study the electrodynamic behavior of actin filaments. Evidence for cable-like properties of actin. Biophys. J., 65: 1371-1378.

27. Tuszynski, J. A., Brown, J. A., Crawford, E., Carpenter, E. J., Nip, M. L. A., Dixon, J. M., and M. V. Satarić. 2005. Molecular dynamics simulations of tubulin structures and calculation of electrostatic properties of microtubules. Math. Comp. Model., 41(10): 1055-1070.

28. Needleman, D. J., Ojeda-López, M. A., Raviv, U., Miller, H. P., Wilson, L., and C. R. Safinya. 2004. Higher-order assembly of microtubules by counterions: from hexagonal bundles to living necklaces. Proc. Natl. Acad. Sci. USA, 101(46): 16099-16103.

bioRxiv preprint doi: https://doi.org/10.1101/2020.04.21.054155; this version posted April 23, 2020. The copyright holder for this preprint (which was not certified by peer review) is the author/funder, who has granted bioRxiv a license to display the preprint in perpetuity. It is made available under aCC-BY-NC-ND 4.0 International license.

29. Zhang, P., and H. F. Cantiello. 2009. Electrical mapping of microtubular structures by surface potential microscopy. Appl. Phys. Lett., 95: 113703.